Electrochemical Deposition of Copper on a Gold Electrode in Sulfuric Acid: Resolution of the Interfacial Structure

Michael F. Toney, Jason N. Howard,* Jocelyn Richer,† Gary L. Borges, Joseph G. Gordon, and Owen R. Melroy
IBM Research Division, Almaden Research Center, San Jose, California 95120

Dennis Yee and Larry B. Sorensen
Department of Physics FM-15, University of Washington, Seattle, Washington 98195
(Received 26 June 1995)

The structure of electrochemically deposited submonolayer Cu on Au(111) in sulfuric acid has been extensively investigated but is still poorly known. We report an x-ray scattering determination of this structure that explains existing data. The Cu adatoms form a honeycomb lattice and are adsorbed on threefold hollow sites, while sulfate anions occupy the honeycomb centers. Three oxygens of each sulfate bond to Cu atoms. This stabilizes the structure and illustrates that anion effects can be important in electrodeposited structures. Our results indicate that previous scanning tunneling and atomic force microscopy measurements imaged the sulfate molecules not the Cu atoms.

PACS numbers: 68.45.–v, 68.55.Jk, 61.10.–i, 82.45.+z

The molecular level structure at electrode-electrolyte interfaces plays a crucial role in interfacial electrochemical processes, such as electrodeposition, corrosion, electrocatalysis, and charge transfer. However, it is only recently that this structure has been accessible to experimental measurement *in situ,* due to the advent of methods such as surface extended x-ray absorption fine structure (EXAFS) [1,2], surface x-ray scattering [3], scanning tunneling microscopy (STM) [4–7], and atomic force microscopy (AFM) [8]. As these methods are brought to bear on increasingly complicated interfaces, it is important to understand these tools, and their limitations and strengths, when applied *in situ* to electrode-electrolyte interfaces. One actively studied area of interfacial electrochemistry where these tools provide significant insight is the electrodeposition of monolayers and submonolayers of metals on foreign metal substrates [9] because of the importance of these layers in adsorption, charge transfer, nucleation and growth, and electrocatalysis.

An archetype of such deposition (known as underpotential deposition or UPD) is Cu on the (111) face of Au in sulfuric acid. The UPD of Cu occurs in two distinct stages, where there is good agreement that the second-stage adsorbed layer forms a full monolayer [1,2,4,10,11]. There is no agreement on the atomic structure of the first stage (or submonolayer) of Cu on Au(111), despite investigations by *in situ* EXAFS [2], STM [4,5,7], AFM [8], *ex situ* surface science methods [12], and other techniques [10,11,13–15]. Two intriguing aspects of UPD Cu/Au(111) make structure determination, and indeed knowledge of the Cu coverage, difficult. One is that, on adsorption, the Cu^{2+} ion is not fully discharged to neutral Cu^0, but carries a charge [2,10,14,15] whose magnitude is not known. Another is that sulfate (SO_4^{-2}) or perhaps bisulphate (HSO_4^-) is coadsorbed with Cu [10–15], and markedly affects the deposition kinetics, and presumably, the structure. Although it is not known if the adsorbed species is sulfate or bisulphate, we refer to it as sulfate.

Ex situ electron diffraction and Auger spectroscopy of first state Cu/Au(111) lead to the proposal of a $(\sqrt{3} \times \sqrt{3})R30°$ lattice with Cu atoms forming a honeycomb structure [Cu coverage of 2/3 monolayer (ML)] [12], but no surface crystallographic measurements were conducted to support this. Although *ex situ* experiments are susceptible to changes in the electrode-electrolyte interface upon removal from solution, this model has been supported recently by microbalance measurements that show most of the Cu monolayer is deposited in the first deposition stage [11] and by chronocoulometric experiments that indicate the Cu and sulfate coverages are about 2/3 and 1/3 ML, respectively [10,13]. In contrast to this, *in situ* STM and AFM images show high contrast features 0.5 nm apart and aligned 30° from the Au lattice [4,5,7,8]. Based on this, a $(\sqrt{3} \times \sqrt{3})R30°$ structure was proposed where the Cu atoms form a simple triangular lattice (0.5 nm Cu-Cu spacing and 1/3 ML Cu coverage).

In this Letter we report *in situ* x-ray scattering measurements that allow a detailed determination of the first stage interfacial structure: a honeycomb lattice of Cu atoms (2/3 ML coverage) with sulfate molecules adsorbed in the centers (1/3 ML coverage) above the plane of Cu atoms. Three oxygen atoms of each sulfate molecule are chemically bonded to Cu atoms, and one points away from the surface. This structure explains existing data, lends insight into STM and AFM imaging mechanisms in an electrolyte, and provides an understanding of the stabilization of this structure.

Our experiments were performed *in situ* [16] with the electrode potential at 0.12 V (vs Cu/Cu^{2+}), corresponding to the first deposition stage. Data were obtained in two experiments at the National Synchrotron Light Source, one on X20A and the other on X20C. The incident x-ray energies were about 10 keV, and the diffracted beam was

 0031-9007/95/75(24)/4472(4)$06.00

analyzed with 1 mrad Soller slits. The electrolyte was $0.1M$ H_2SO_4 containing 2.5mM $CuSO_4$ and was prepared from ultrapure reagents (Johnson-Mathey) and high-pressure liquid chromatography deionized water. Au(111) single crystals were prepared by successive mechanical polishing to a grit size of 0.3 μm, followed by annealing at 700 to 800 °C for several days. Just prior to use, the Au(111) surface was treated by either (i) annealing in the oxidizing flame of a propane torch [17] or (ii) electropolishing [18] with a final cleaning in ozone. In both cases, characteristic current-voltage curves for Cu/Au(111) [5,7,10–12] were obtained prior to the x-ray experiments.

Figure 1(a) shows the in-plane diffraction pattern for Cu/Au(111). The solid symbols represent Bragg diffraction rods [3,19] that we measured, while the open symbols are symmetry related rods. The squares are fractional order rods, which are due only to the Cu adlayer, while the circles are integral order rods and have intensities that depend on the adlayer and substrate structures. The diffraction pattern shown that the adlayer has $(\sqrt{3} \times \sqrt{3})R30°$ periodicity, consistent with the previous observations. We never observed a (5×5) structure, which is reportedly stabilized by chloride contamination [5]. The atomic structure is determined from the diffracted intensities measured along the Bragg rods. Figures 1(b)–1(d) and 2 show integrated intensity profiles of the fractional and integral rods, respectively. They have been corrected for instrumental effects [20], and the fractional order rod data [Figs. 1(b)–1(d)] have been converted into absolute (electron) units. Data are plotted as a function of Q_z, the component of the scattering vector normal to the Au(111) surface.

From these data we can immediately rule out the triangular $(\sqrt{3} \times \sqrt{3})R30°$ structure proposed in the STM and AFM experiments. Such a flat adsorbed layer would have fractional order profiles that are about three times as intense as the data in Figs. 1(b)–1(d) and that fall off slowly with Q_z, due to a decreasing Debye-Waller factor and Cu atomic form factor. Since the intensity of the fractional order rods do not monotonically decrease with Q_z, the adlayer structure must consist of atoms of different heights above the Au(111) surface. From this and the likely coadsorption of sulfate molecules, we considered models with both ordered Cu and sulfates. In addition, the small

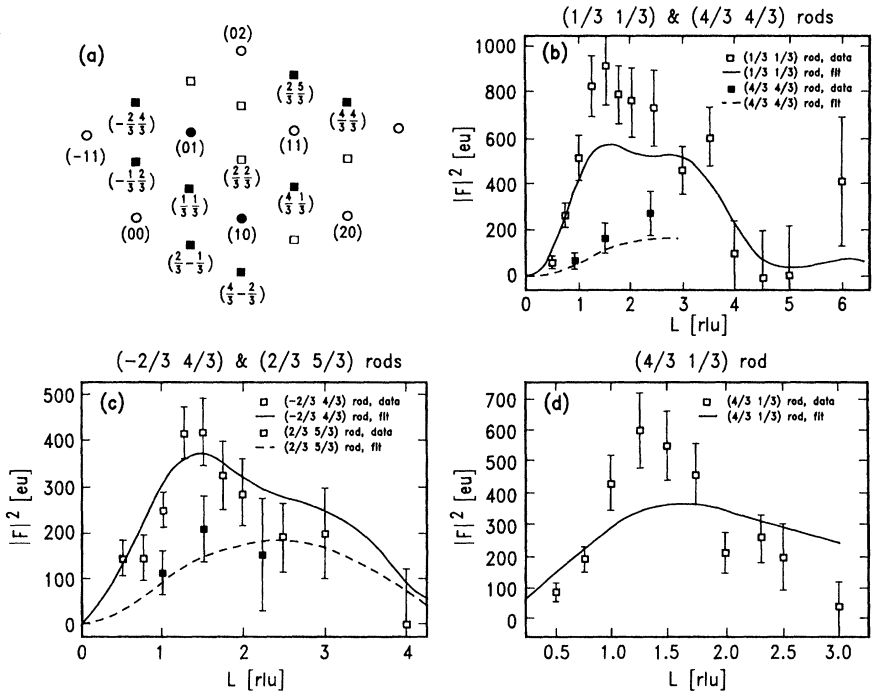

FIG. 1. Diffraction data for Cu/Au(111) at the first deposition stage. (a) In-plane diffraction pattern. The solid symbols represent Bragg rods that were measured, while the open symbols are symmetry related rods that were not. The squares are fractional order rods, while the circles are integral order rods. (b) Structure factors for the (1/3 1/3) and (4/3 4/3) rods, open and closed squares, respectively. The abscissa is in reciprocal lattice units (1 rlu = 8.9 nm^{-1}). (c) Structure factors for the (−2/3 4/3) and (2/3 5/3) rods, open and closed squares, respectively. (d) Structure factor for the (4/3 1/3) rod. These data have been converted into absolute units (to an accuracy of about 20%). In the diffraction (ϕ) scans used to calculate these integrated intensities, the peak intensities are small, and the backgrounds are large and vary with ϕ. As a result the backgrounds cannot be accurately determined, and the error bars are large. In (b)–(d) the lines are the best fit to the data using the structure shown in Fig. 3. To fit these and the data in Fig. 2, we allowed the following to vary: Cu-Au plane spacing, Cu-S spacing, spacing between sulfur and outward pointing oxygen, spacing between sulfur and inward pointing oxygens, occupancy of sulfates, and one (constrained) scale factor. All Debye-Waller factors were fixed at 0.01–0.02 nm, but varying these does not affect our results.

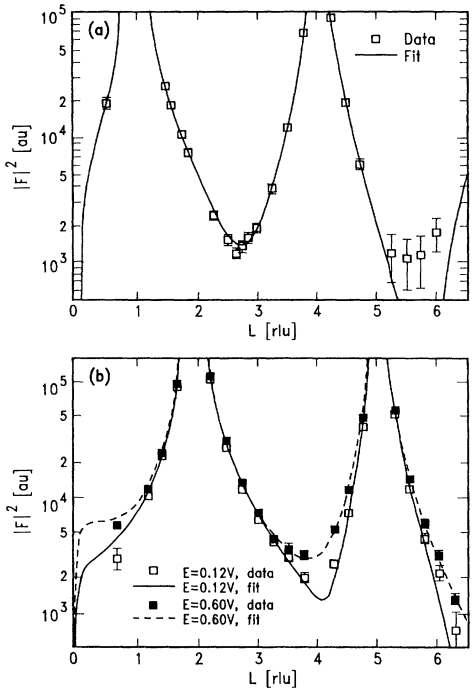

FIG. 2. Structure factors for the (10) and (01) Bragg rods, (a) and (b), respectively. The open squares are for Cu/Au(111) at the first deposition stage ($V = 0.12$ V), while the filled circles are for a clean Au(111) surface ($V = 0.60$ V, where no ordered Cu or sulfate is adsorbed). The data have been approximately converted into absolute units (within a factor of about 10). The solid line is the best fit to the 0.12 V data using the interfacial structure shown in Fig. 3, while the dashed line is the best fit to the 0.60 V data. The scale factor and surface roughness [19,20] were obtained from this latter fit.

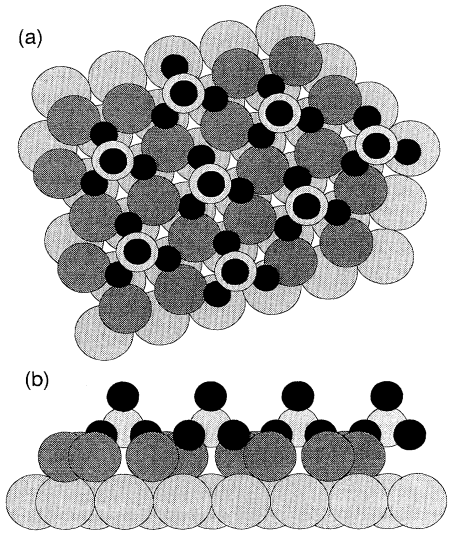

FIG. 3. Interfacial structure of Cu/Au(111) at the first deposition stage. (a) Top view. (b) Side view. The large light gray, medium gray, small light gray, and filled spheres represent gold, copper, sulfur, and oxygen atoms, respectively.

intensities for the (1/3 1/3) and (−2/3 4/3) rods at $Q_z \simeq 0$ points to a structure containing two Cu atoms and one sulfate molecule with each spaced about one Au surface lattice constant apart. This is because in such an adsorbed layer structure the scattering amplitude of these rods at $Q_z \simeq 0$ is proportional to that of a Cu atom minus that of a sulfate molecule, and for these scattering vectors, the amplitudes are approximately equal and subtract to zero. Thus, we considered models based on this motif.

In the quantitative determination of the adlayer structure, both the fractional and integral rod intensities [Figs. 1(b)–1(d) and 2] were fit simultaneously by structural models using a least-squares method. This allows a determination of the adlayer structure and its registry with the substrate. We note that for the integral rods (Fig. 2) the scale factor and surface roughness [19,20] were obtained from an independent fit to the data at 0.60 V [dashed lines in Fig. 2(b)], where no adsorbed Cu layer is formed. The model giving the best fit is shown in Fig. 3 and has a goodness of fit $\chi^2 = 2.0$. The Cu atoms form a honeycomb lattice (2/3 ML coverage), and sulfate molecules are adsorbed in the honeycomb centers above the Cu atoms and have (85 ± 15)% occupancy. Both Cu atoms and sulfate molecules occupy face-centered cubic (fcc) threefold hollow sites on the Au(111) surface. Three oxygen atoms of each sulfate molecule are bonded to Cu atoms, and the remaining oxygen points away from the surface. This structure will be discussed below, but we first consider the reliability of our structure determination. First, we tried to fit the data by models having different degrees of sulfate rotational disorder. Adequate fits could not be obtained for either isotropic free rotation or free rotation about the surface normal with one oxygen pointing either away from or into the surface (in all cases, $\chi^2 > 8$). In addition, the bonding configuration shown in Fig. 3, oxygens pointing between Cu atoms and above the surface Au atoms, was the only one capable of providing a suitable description of the data (i.e., $\chi^2 < 3$). Since the Cu atoms are not in symmetric sites, we also considered the possibility of slight displacement of these from fcc hollows, i.e., pairing of Cu atoms toward or away from the bonding oxygens atoms. Such pairing did not produce significantly better fits to the data, and we conclude that any displacements are less than 0.02 nm. Finally, we considered other adsorption sites for the adsorbed Cu and sulfates (e.g., hexagonal close packed hollows, bridge sites, and atop sites), but all produced unacceptable fits ($\chi^2 \gtrsim 20$).

From the structural model (Fig. 3), several bond lengths and plane spacings are calculated and shown in Table I. The bond length between the Cu adatoms and the inward-pointing O atoms (0.215 nm) is typical of Cu-O bond lengths in inorganic compounds [21,22]. This provides the first clear evidence that the sulfate molecules are chemically bonded to the Cu adatoms. This bond likely stabilizes the partial charge on the Cu adatoms and the open structure shown in Fig. 3. Such a structure is not found in

TABLE I. Structural parameters for Cu/Au(111).

Cu-O bond length	0.215 ± 0.02 nm
Cu-S plane spacing	0.149 ± 0.01 nm
Au-S plane spacing	0.376 ± 0.01 nm
Au-Cu plane spacing	0.227 ± 0.005 nm
Au-Cu atomic spacing	0.281 ± 0.005 nm
SO_4 occupancy	0.85 ± 0.15
S-O bond length, top O	0.155 ± 0.02 nm
S-O bond length, O bonded to Cu	0.14 ± 0.02 nm
S-O bond length in SO_4	0.145 nm

vacuum deposition of Cu on Au(111) [23] nor in electrodeposition of Cu on Au(111) in perchlorate, a nonadsorbing electrolyte [8,12]. Thus, the anion is a *crucial participant* in the adlayer structure and its formation, as has been seen for several other electrochemically deposited adlayers [24]. The best fit yields an (85 ± 15)% occupancy of the sulfate molecules. This less than complete occupancy is qualitatively consistent with chronocoulometric data [10] and with STM data, which show antiphase domain boundaries and sulfate point vacancies [4,7]. The expected spacing between the Cu adatoms and surface Au(111) atoms is the sum of the average metallic radii of Au and Cu, 0.272 nm. The observed 0.281 nm Cu-Au spacing is larger than this, which may result from the sulfate coadsorption or the partial charge on the Cu adatoms. Finally, we note that our structural model is consistent with the model assumed by Huckaby and Blum [25] in their theoretical study of metal UPD.

Our model permits an interpretation of the STM and AFM data that is consistent with other information on this system. Recall that STM and AFM imaged high contrast features 0.5 nm apart and aligned 30° from the Au lattice, leading to the proposal of a triangular $(\sqrt{3} \times \sqrt{3})R30°$ structure with 1/3 ML Cu coverage [4,5,7,8]. The sulfate ions in our model have the same periodicity as the features in the STM/AFM images and protrude well above the plane of Cu adatoms. Thus, it is these molecules that are images, not the Cu adatoms. This conclusion is surprising, since one expects sulfate molecules to conduct more poorly than Cu atoms and to be weakly bonded to the surface and hence mobile. That sulfate is "attached" to the surface strongly enough to be imaged supports our conclusion that it is bonded to the Cu adatoms. Recently, STM images of sulfate molecules on Au(111) have been reported in the absence of Cu [6,26], and although the exact structure is controversial, this further strengthens our interpretation that the STM images sulfate for Cu/Au(111). Our results highlight the caution that must be exercised in the interpretation of the STM and AFM images in an electrolyte.

This work was partially supported by the Office of Naval Research. It was performed at the National Synchrotron Light Source, Brookhaven National Laboratory, which is supported by the U.S. Department of Energy. We thank Jean Jordan-Sweet and René Holaday for their assistance with X20.

*Present address: Energy Products Division, Motorola, Lawrenceville, GA 30243.
†Present address: Center for Nuclear Energy Research, University of New Brunswick, Fredericton, NB E3B 6C2 Canada.

[1] O. R. Melroy, M. G. Samant, G. L. Borges, J. G. Gordon, L. Blum, J. H. White, M. J. Albarelli, M. McMillan, and H. D. Abruna, Langmuir **4**, 728 (1988).
[2] A. Tadjeddine, D. Guay, M. Ladouceur, and G. Tourillon, Phys. Rev. Lett. **66**, 2235 (1991).
[3] M. F. Toney and O. R. Melroy, in *Electrochemical Interfaces: Modern Techniques for In-Situ Interface Characterization,* edited by H. D. Abruna (VCH Verlag Chemical, Berlin, 1991), pp. 57–129.
[4] O. M. Magnussen, J. Hotlos, R. J. Nichols, D. M. Kolb, and R. J. Behm, Phys. Rev. Lett. **64**, 2929 (1990).
[5] O. M. Magnussen, J. Hotlos, G. Beitel, D. M. Kolb, and R. J. Behm, J. Vac. Sci. Technol. B **9**, 969 (1991).
[6] G. J. Edens, X. Gao, and M. J. Weaver, J. Electroanal. Chem. **375**, 357 (1994).
[7] T. Hachiya, H. Honbo, and K. Itaya, J. Electroanal. Chem. **315**, 275 (1991).
[8] S. Manne, P. K. Hansma, J. Massie, V. B. Elings, and A. A. Gewirth, Science **251**, 183 (1991).
[9] D. M. Kolb, in *Advances in Electrochemistry and Electrochemical Engineering,* edited by H. Gerischer and C. W. Tobias (Wiley, New York, 1978), Vol. 11, p. 125.
[10] Z. Shi and J. Lipkowski, J. Electroanal. Chem. **365**, 303 (1994).
[11] G. L. Borges, K. K. Kanazawa, J. G. Gordon, K. Ashley, and J. Richer, J. Electroanal. Chem. **364**, 281 (1994).
[12] M. S. Zei, G. Qiao, G. Lehmpfuhl, and D. M. Kolb, Ber. Bunsen-Ges. Phys. Chem. **91**, 349 (1987).
[13] Z. Shi and J. Lipkowski, J. Electroanal. Chem. **364**, 289 (1994).
[14] P. Zelenay, L. M. Rice-Jackson, and A. Wieckowski, Surf. Sci. **256**, 253 (1991).
[15] I. H. Omar, H. J. Pauling, and K. Jüttner, J. Electrochem. Soc. **140**, 2187 (1993).
[16] M. F. Toney, J. G. Gordon, M. G. Samant, G. L. Borges, O. R. Melroy, D. Yee, and L. B. Sorensen, Phys. Rev. B **45**, 9362–9374 (1992).
[17] J. Clavilier, J. Electroanal. Chem. **107**, 211 (1980).
[18] K. M. Robinson, I. K. Robinson, and W. E. O'Grady, Electrochem. Acta **37**, 2169 (1992).
[19] R. Feidenhans'l, Surf. Sci. Reports **10**, 105–188 (1989).
[20] M. F. Toney and D. G. Wiesler, Acta Crystallogr. Sect. A **49**, 624 (1993).
[21] G. M. Brown and R. Chidambaram, Acta Crystallogr. Sect. B **25**, 676 (1969).
[22] G. M. Brown and R. Chidambaram, Acta Crystallogr. Sect. B **29**, 2393 (1973).
[23] Y. Nakai, M. S. Zei, D. M. Kolb, and G. Lehmpfuhl, Ber. Bunsen-Ges. Phys. Chem. **88**, 340 (1984).
[24] C. Chen, S. M. Vesecky, and A. A. Gewirth, J. Am. Chem. Soc. **114**, 451 (1992).
[25] D. A. Huckaby and L. Blum, J. Electroanal. Chem. **315**, 255 (1991).
[26] O. M. Magnussen, J. Hagebock, J. Hotlos, and R. J. Behm, Discuss. Farraday Soc. **94**, 329 (1992).

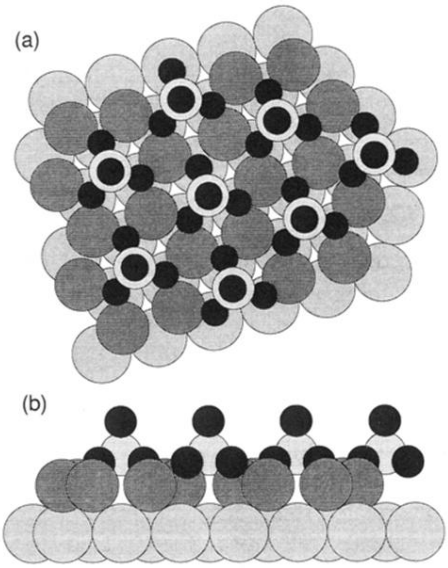

FIG. 3. Interfacial structure of Cu/Au(111) at the first deposition stage. (a) Top view. (b) Side view. The large light gray, medium gray, small light gray, and filled spheres represent gold, copper, sulfur, and oxygen atoms, respectively.